2018 EAGE ANNUAL
80TH CONFERENCE + EXHIBITION
COPENHAGEN | DENMARK

Th P3 11

Data-Windowing Hierarchy in Multi-Parameter Elastic FWI: 3D Synthetic Foothills Case Study

P. Trinh* (Total E&P, ISTerre - Univ. Grenoble Aples), R. Brossier (ISTerre - Univ. Grenoble Aples), L. Metivier (ISTerre - Univ. Grenoble Aples, CNRS, LJK - Univ. Grenoble Aples), J. Virieux (ISTerre - Univ. Grenoble Aples)

Summary

Full waveform inversion (FWI) in onshore targets remains very challenging due to the complex free-surface-related effects and 3D geometry representation. In such areas, the seismic wavefield is dominated by highly energetic and dispersive surface waves, converted waves and back-scattering energy. We use a time-domain spectral-element-based approach for elastic wavefield simulation in complex foothill area. The structurally-based nonstationary and anisotropic Bessel smoothing filter is considered for gradient preconditioning to stabilize the inversion, and further constraint the model parameters estimation. The challenges of the elastic multi-parameter FWI in complex land areas are highlighted through a 3D subset of the SEAM Phase II Foothills benchmark. As the data is dominated by surface waves, it is mainly sensitive to the S-wave velocity. We then propose a two-step data-windowing hierarchy to simultaneously invert for P- and S-wave speeds, focusing on early body waves before considering the whole data. By doing so, we exploit the maximum amount of information in the observed data and get a reliable model parameters estimation. Surface waves can be treated as an additional source of information, to provide better constraints on both P- and S-wave velocities estimation at near-surface. Appropriate preconditioning design helps to enhance the model parameters estimation.

Introduction

Full waveform inversion (FWI) for onshore targets remains very challenging due to complex free-surface-related effects and 3D geometry representation (Huiskes et al., 2017). In such areas, the seismic wavefield is dominated by highly energetic and dispersive surface waves, converted waves and back-scattering energy when the waves hit the steep slopes at the surface, or strong velocity contrasts. These complex effects cannot be fully removed or compensated by data pre-processing, implying that a correct description of the physics is strongly advisable for accurate model parameters estimation. Moreover, considering the complete physical phenomena of the wave propagation would make possible to take benefit of each piece of recorded data, for expected more accurate results and higher resolution. Adequate regularization and preconditioning strategies are also required to mitigate the ill-posedness of the inversion problem, especially when dealing with complex structures or geological heterogeneities (Guitton et al., 2012).
In this study, we investigate the challenge of multi-parameter reconstruction in a 3D elastic subtarget of the SEAM Phase II foothills benchmark (Regone et al., 2017). We use the code SEM46 (Spectral Element Method for Seismic Imaging in eXploration), based on a time-domain spectral element method (SEM), for elastic wavefield simulation. The code uses a flexible Cartesian-based deformed mesh with high-order geometry representation to capture complex topographies and variable element-size to reduce the numerical cost (Trinh et al., 2018). The modeling kernel is optimized in the same way as standard SEM approaches (Deville et al., 2002). The inversion is based on the minimization of the least-squares norm between the observed and the calculated data. The structurally-based nonstationary and anisotropic Bessel smoothing filter, directly implemented on the SEM mesh, is considered for gradient preconditioning (Trinh et al., 2017). The filter shape is defined by variable coherent lengths: L_v is associated with the direction perpendicular to the local bedding plan, L_u and L_w are related to the planar structure of potential geological features. The 3D orientation is controlled by azimuth and dip angles. In this paper, we will highlight the importance of data hierarchy and gradient preconditioning to make a successful elastic 3D FWI.

3D elastic case study: Subset of the SEAM foothills benchmark

We consider an isotropic elastic example coming from a 3D subtarget of the SEAM Phase II Foothill model (Regone et al., 2017). The topography variation is significant in this model, with a maximal vertical variation of 800 m as shown in Figure 1. The bedding plans are gently dipping in the x-direction with folding structures, which can be seen from the depth section in Figure 4(a). The model also has an unconformity at 2-3 km depth, which might be difficult to recover by FWI. The velocity attribute extracted at 20 m below the free-surface in Figure 3(a) shows interesting features with complex geometry that FWI aims to reconstruct. We use a 3D surface acquisition with 4 source-lines, each line including 20 sources. The source positions are indicated by black triangles in Figure 1, with inline and crossline source-spacing ΔS_x and ΔS_y taken at 300 m and 500 m, respectively. For each source, a grid of 3-component (3C) receivers is deployed on the whole surface, the distance between two adjacent receivers being 12.5 m. We use vertical point-force. The source-time function is a Ricker wavelet, centered at 3.5 Hz. The total recording time is equal to 6 sec.

Inversion setup

SEM is used for both forward and inversion problems. The observed data is generated with a constant element-size mesh, whereas the inversion problem is computed over a variable element-size mesh, locally satisfying the volume condition. The SEM mesh id deformed by 4^{th}-order shape functions to describe rapid topography variations of the surface (Trinh et al., 2018). The seismic wavefield is complex, including highly energetic and dispersive surface waves due to the rapidly varying topography. Significant back-scattering of body and surface waves as well as mode conversions occur at steep-slope

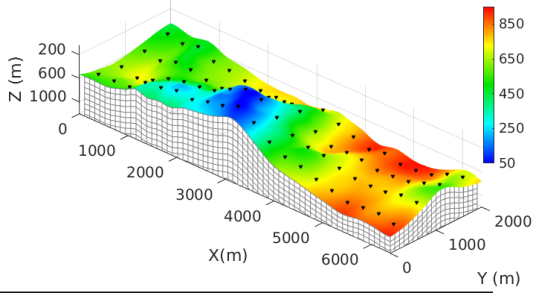

Figure 1: 3D acquisition design superimposed on the topography map, where the colorbar illustrates the absolute depth Z_{abs}(m) from a pre-defined zero-depth: Sources positions are marked by black triangles $\Delta S_x = 320$ m, $\Delta S_y = 500$ m.

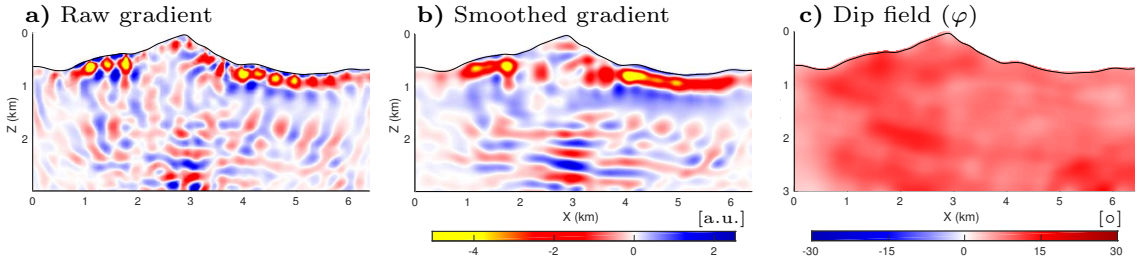

Figure 2: Gradient smoothing illustration underneath the source line at $Y = 750$ m: (a) Original scaled gradient without any smoothing, showing significant acquisition footprint and artifacts due to sparse acquisition. (b) Smoothed gradient by Bessel filter. (c) Smooth dip field used for the smoothing filter.

surface positions.
The initial V_p, V_s models are smoothed versions of the true model (Figures 3(b)). Similar smoothed model is used for density as the input of the inversion process. To investigate on different aspects of elastic FWI, such as gradient preconditioning and data-windowings hierarchy, we choose here a set of starting models compatible with the frequency-content of the data: the calculated data is not cycle-skipped compared with the observed data. We invert simultaneously for V_p and V_s, and the density is kept unchanged. Each inversion sequence consists of 60 iterations of the l-BFGS optimization method. We do not apply other preconditioning or regularization than the Bessel gradient smoothing as detailed below.

Structure-oriented gradient preconditioning

The raw gradient computed in the initial model is presented in Figure 2(a), showing significant acquisition footprint at the near-surface. Unrealistic oscillations also occur at greater depths, due to the limited illumination coming from the sparsity of the sources. However, the targets have considerable dipping and folding structures, which can be characterized by smooth azimuth and dip fields as shown in Figures 2(c). The 3D orientation can be obtained from migrated images or geological prior information. The structures vary quicker in the vertical direction than the horizontal directions, we thus design an anisotropic filter: vertical coherent length $L_v = 25$ m; for other directions, the value of L_u and L_w increases from 25 m near the unconformity position to 100 m elsewhere. As a result, the filter has an isotropic shape near the unconformity to avoid any smearing effect across the unconformity.
By considering these filter parameters in the structure-oriented Bessel preconditioning, we obtain the smoothed gradient 2(b): The artifacts due to the acquisition footprint and the poor illumination are effectively attenuated, without degrading the deeper structures. The continuity of the features at greater depths is enhanced since the oscillations are reduced. We also obtain a correct orientation of the geological features coming from the design of the 3D rotation. The smoothing process costs only 0.4% running time of one FWI iteration.

Data-windowing hierarchy

If we use all the data as the input for the inversion, all the updates will go to V_s as is discussed in the following section. To mitigate this effect, we propose a two-step data-windowing hierarchy where the models are first inverting with early-body waves, arriving before the surface waves. The observed models will then be used as starting models for the inversion will all the wavefield. We simply use a time-windowing to separate the early-body waves with the surface waves and underlying reflected and back-scattering waves.

Results and discussion

The results obtained after the first step (inversion of early-body waves only) are shown in cross-section 3(c). The inversion successfully recovers the main structures of the V_p model. The reconstruction of the V_s model is limited at 2 km depth due to the shallow penetration of the shear component. The models presented in Figures 3(c) and (d) are obtained after the second step, accounting for the whole dataset. Adding surface waves and other parts of the wavefield does not degrade the V_p estimation and improve significantly the V_s model. The continuity of the near-surface features are strengthened and the deeper structures are better resolved. The unconformity is well reconstructed in the V_s model at 2 km depth (Figure 3(d) right panel). This is in part due to the nonstationary design of the Bessel filter.

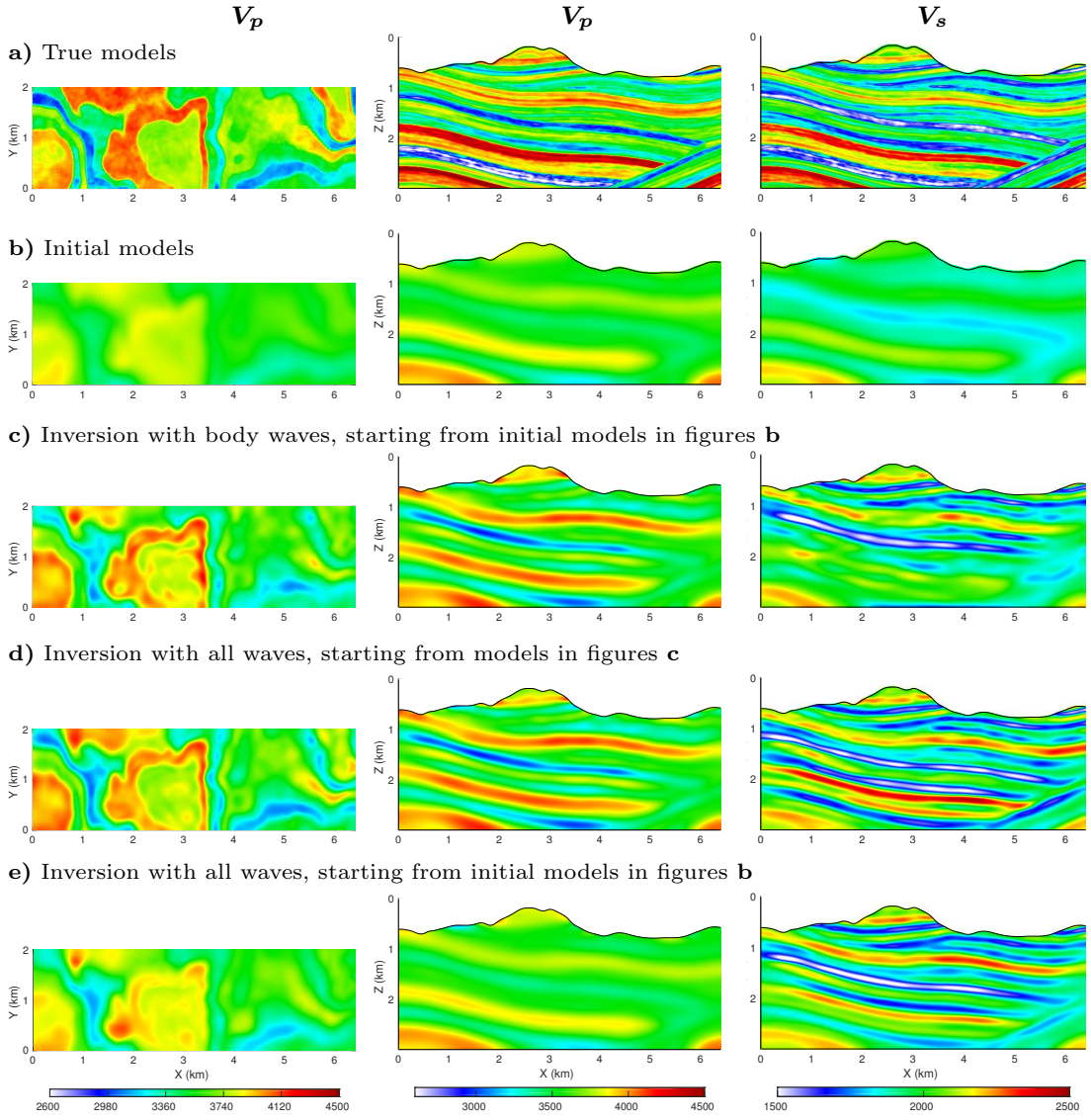

Figure 3: Left - V_p velocity attribute extracted at 20 m below the free-surface. Middle and right - V_p and V_s cross-sections at $Y = 1$ km: (a) True models. (b) Initial models. (c) Inversion results by only using the early-body waves, starting from the initial models. (d) Inversion results by using all the wavefield, starting from models in figure (c), showing significant improvement for the V_s estimation. (d) Inversion results by using all the wavefield, starting from the initial models - insignificant update in V_p estimation.

When looking at the velocity attributes extracted at 20 m below the free-surface (Figures 3(c) and (d)), inverting for surface waves actually improves the thin-structure imaging and amplitude estimation for both V_p and V_s.

Importance of the data-windowing hierarchy

Since the calculated data from the initial models is not cycle-skipped compared with the observed data, one can run the inversion will all the data, without any distinction between body and surface waves. The inverted results are shown in Figure 3(e), where the V_s model is well-reconstructed. However, we observe insignificant updates of the V_p model: as the data is dominated by surface waves, the least-squares misfit function is mainly sensitive to V_s. By focusing on early body waves before considering the whole data, our data-windowing hierarchy make possible to better constrain the P-wave velocity. For complex real data applications, especially in foothill environment, this data separation between early body waves and surface waves might be difficult to achieve. In such a case, a model hierarchy could be used on top of this data-windowing strategy, where Bessel gradient preconditioning and/or model regularization could be used to monitor the wavenumber-content of the allowed model updates. At the first step, only

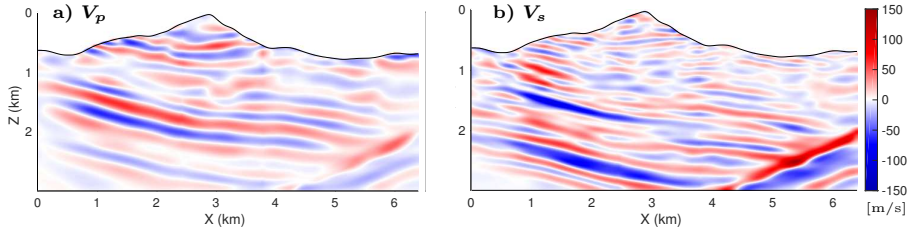

Figure 4: Difference between inverted results with structure-oriented preconditioning (Fig. 3(d)) and the inversion results with stationary smoothing $L_v = 25$ m, $L_u = L_w = 100$ m, 0° dip and azimuth angles. (a) and (b) are V_p and V_s cross-sections at $Y = 750$ m. The rotational gradient preconditioning mainly affects the amplitude estimation.

low-wavenumber V_s updates would be allowed in order to build a reliable V_p estimation.

Structure-oriented Bessel preconditioning enhances the model estimation

Figure 4 shows the difference between inverted results with the nonstationary structure-oriented preconditioning and the inversion with the stationary filter (coherent lengths $L_v = 25$ m, $L_u = L_w = 100$ m, and 0° dip and azimuth angle), under the same inversion hierarchy and setting. The comparison shows a nonnegligible modification of the amplitude estimation for both V_p and V_s, especially following the dipping directions. In particular, a significant difference can be observed at the unconformity because the nonstationary filter is reduced to isotropic shape near this location. The model update is thus not smeared out across the unconformity, leading to a sharp interface as shown in the final V_s model in Figure 3(d). It should be noted that we only impose the relative position of the unconformity, and we simply reduce the filter effect at this location. By doing so, the filter does not artificially sharpen the interface but let FWI free to reconstruct it.

Conclusions

The paper illustrates the complexity of the data and elastic multi-parameter FWI problem in complex land areas even with a relatively accurate starting models. We propose a two-step data-windowing hierarchy to simultaneously invert for V_p and V_s in order to get a reliable model parameters estimation, but also to exploit the maximum amount of information in the observed data. Surface waves can be treated as an additional source of information, to provide better constraints on both V_p and V_s estimation at near-surface. Appropriate preconditioning also helps to enhance the model parameters estimation. Perspectives include elastic and visco-elastic application on different acquisition configurations on large-scale complex land targets, where alternative misfit function might play an important role.

Acknowledgements

The authors would like to thank Total E&P for financial support of PTT's PhD project, and for allowing to present and access the SEAM Phase II Foothills model. This study was partially funded by the SEISCOPE consortium (*http://seiscope2.osug.fr*), sponsored by AKERBP, CGG, CHEVRON, EXXON-MOBIL, JGI, PETROBRAS, SCHLUMBERGER, SHELL, SINOPEC, STATOIL and TOTAL. This study was granted access to the HPC resources of CIMENT infrastructure (https://ciment.ujf-grenoble.fr) and CINES/IDRIS/TGCC under the allocation 046091 made by GENCI.

References

Deville, M., Fischer, P. and Mund, E. [2002] *High Order Methods for Incompressible Fluid Flow*. Cambridge University Press.

Guitton, A., Ayeni, G. and Díaz, E. [2012] Constrained full-waveform inversion by model reparameterization. *Geophysics*, **77**(2), R117–R127.

Huiskes, M., Plessix, R. and Mulder, W. [2017] Acoustic VTI Full-waveform Inversion with 3-D Free-surface Topography. In: *79th Annual EAGE Meeting (Paris)*.

Regone, C., Stefani, J., Wang, P., Gerea, C., Gonzalez, G. and Oristaglio, M. [2017] Geologic model building in SEAM Phase II - Land seismic challenges. *The Leading Edge*, **36**(9), 738–749.

Trinh, P.T., Brossier, R., Métivier, L., Tavard, L. and Virieux, J. [2018] Efficient 3D time-domain elastic and viscoelastic Full Waveform Inversion using a spectral-element method on flexible Cartesian-based mesh. *Submitted to Geophysics*.

Trinh, P.T., Brossier, R., Métivier, L., Virieux, J. and Wellington, P. [2017] Bessel smoothing filter for spectral element mesh. *Geophysical Journal International*, **209**(3), 1489–1512.